International Journal of Emerging Science and Engineering (IJESE)
ISSN: 2319–6378 (Online), Volume-13 Issue-2, January 2025

Dynamic Response of Suspension Bridges Due to Coupling Between Buffeting and Aeroelastic Flutter

Hafid Mataich, Bouchta El Amrani

Abstract: ***The effects of turbulent winds on suspension bridges are considerable, significantly influencing the bridge's floating instability and, as a result, its safety and performance. Predicting the coupled response of buffeting and flutter in suspension bridges is an advanced area of structural and aeroelastic engineering. Buffeting and flutter are not independent phenomena; buffeting, by exciting specific natural frequencies of the bridge, can contribute to the onset of flutter. Furthermore, once flutter is triggered, it alters the dynamics of the bridge, potentially amplifying the effects of buffeting. The interaction between these two phenomena can lead to complex dynamic responses that are challenging to predict through separate analyses. This paper explores this phenomenon in the time domain, requiring the expression of aerodynamic forces via convolution integrals, which incorporate the aerodynamic impulse function, structural motions, and wind fluctuations. We analyzed the aerodynamic response of the old Tacoma Bridge in the USA, situated on complex terrain and subjected to turbulent winds. A formulation that accounts for the lateral, vertical, and torsional motions of the bridge deck structure was used. The Beta-Newmark numerical algorithm was employed to integrate the bridge's time response. Subsequently, parametric studies were conducted to further elucidate the concepts of buffeting-flutter coupling in long-span suspension bridges, aiming to assist designers in developing effective control protocols.***

Keywords: Suspension Bridge; Aeroelastic Instability; Wind Turbulence; Buffeting; Flutter

I. INTRODUCTION

Predicting the coupled response of buffeting and flutter in suspension bridges is an advanced field of structural and aeroelastic engineering. The coupling of these two phenomena, buffeting (random excitation due to wind turbulence) and flutter (self-sustained instability due to aerodynamic interactions), is crucial to understanding the combined effects on the stability and durability of suspension bridges. Buoyancy-buffeting coupling is a complex aerodynamic phenomenon that occurs in structures subjected to turbulent winds, notably suspension bridges. This coupling combines two distinct types of dynamic response to wind action, buffeting and flutter [1]. Researchers Yi et al (2022) and Brownjohn and Jakobsen (2001) have defined flutter in suspension bridges as a self-sustaining aerodynamic instability that occurs when the wind speed reaches a critical value [2]. Above this speed, the aerodynamic forces are no longer damped by the internal forces of the structure (such as structural damping and stiffness), resulting in increasing oscillations. These oscillations can become catastrophic if left unchecked [3]. While Defang et al. (2024) and Lorenzo et al. (2023) have described buffeting as the response of the structure to wind gusts [4]. Unlike flutter, buffeting is a forced response, where the structure oscillates under the effect of random variations in wind speed. This oscillation can occur at wind speeds below the critical floating speed, as they show Zhang et al. (2021) [5], Hua et al. (2020) [6].

Complex topography, such as mountains, valleys and seas, all influence the overall wind speed in the atmospheric layer where bridges are built. What's more, in the real world, we can't assume that the wind is laminar or uniform. Consequently, the deviation of wind speed variations around its mean value must be taken into account in the aerodynamic formulation of the problem. The effect of these wind speed variations is a type of structural vibration known as buffeting. New cable-stayed bridges, also known as long-span suspension bridges, are generally very sensitive to random wind excitations. Buffeting loads on bridge structures can vary considerably due to turbulence in the atmospheric boundary layer, as described by Xia and Ge (2020) [7]. The amplitude of the most energy-loaded wind vortices in the vortex fluctuation field is expressed by an important parameter called the turbulence integral scale, Mataich and El Amrani (2023) [8]. The latter factor has an effect on buffeting loads and, consequently, on the dynamic behavior of bridges installed in topographic sites where atmospheric turbulence is strong, as shown by Li et al. (2021) [9]. Hu and Xu (2014) [10], Tang et al. (2017) estimated that buffeting is a type of forced and random vibratory motion produced by the suspension bridge under the action of fluctuations in mean wind speed [11]. Thus, the buffeting vibration of bridges is the result of excitation by low wind speeds. In reality, these random vibrations do not pose a problem in terms of aeroelastic instability of the bridge structure, but they can lead to fatigue failure of the bridge structure, which poses maintenance problems, as shown in the study by Shuyang and Jinxin (2017) [12]. Mataich et al. (2024) studied the dynamic behavior of the suspension bridge subjected to float-buffeting coupling, but in the frequency domain [13].

The old Tacoma Bridge, shown in its topographic site in figures 1 and 2, is considered the most modern bridge of its time in terms of engineering and design. It was inaugurated in 1940 in the USA, but only operated for just over three months before collapsing in a manner that shocked

Manuscript received on 24 August 2024 | First Revised Manuscript received on 26 December 2024 | Second Revised Manuscript received on 03 January 2025 | Manuscript Accepted on 15 January 2025 | Manuscript published on 30 January 2025.
*****Correspondence Author(s)
Hafid Mataich*, Laboratory of Mathematics, Modeling and Applied Physics, Higher Normal School, Sidi Mohamed Ben Abdellah University, Fez, Morocco. Email ID: hafid.mataich@usmba.ac.ma, ORCID ID: 0009-0009-9210-5603.
Prof. Bouchta El Amrani, Laboratory of Mathematics, Modeling and Applied Physics, Higher Normal School, Sidi Mohamed Ben Abdellah University, Fez, Morocco. Email ID: bouchta.elamrani@usmba.ac.ma.

everyone, including engineers and designers. Specialists investigated the possible reasons for this shocking collapse, and all agreed that there was a design flaw that didn't take aerodynamic factors into account, as shown by Fenerci et al. (2017) [14]. Indeed, on the day of its collapse, it was observed to vibrate vertically according to Cheynet et al. (2016) [15], then unexpectedly generate torsional oscillations that rapidly coupled with the wind, causing the amplitude of these oscillations to increase until it finally collapsed as shown by Weichao et al. (2024) [16], Arioli and Gazzola (2017) [17], Ammann et al. (1941) [18]. The question that has been raised ever since is how the oscillations went from vertical to torsional. There are many explanations for this phenomenon, but no one has investigated the possibility of linking the phenomenon of vertical flutter oscillations to the random nature of the wind, which is the focus of this research.

[Fig.1: Map of Tacoma and positioning of its bridge in the United States] [17]

[Fig.2: Old Tacoma Suspension Bridge] [18]

Yes, that's right. We don't have stochastic wind data for Tacoma Bay. As a reminder, the aim of this study is to determine the effect of turbulent winds in the time domain on the stability of the suspension bridge structure. Therefore, we will only generate records for turbulent winds based on the numerical method.

II. MATHEMATICAL FORMULATION OF THE COUPLING PROBLEM

Time-domain coupling of flutter and buffeting is an approach that captures the complex dynamic interactions between these two aeroelastic phenomena in real time, by simulating their simultaneous evolution under the influence of variable aerodynamic forces.

A. Formulation Assumptions

In this section [19], the assumptions and approximations that form the basis of this work are inspired by the framework of Scanlan (1978) and Scanlan (1982) as follows

- Quasi-stationarity: Wind fluctuations adapt instantaneously to the moving bridge deck [20].
- Linearity: Based on Taylor expansion to order 1, we neglect the higher-order terms of the aerodynamic forces. As such, aerodynamic damping is assumed to vary linearly with mean wind speed.
- Modal coupling: Based on wind speed records of less than 50 m/s, we assume that there is no structural modal coupling.
- To ensure that wind vortices do not deform as they cross the suspension bridge, we assume that the structural width of the suspension bridge is less than the length of the wind turbulence.

B. Coupled Bridge-Wind Equation of Motion

Currently, two techniques have been used to obtain the buffeting response of suspension bridges: experimental wind tunnel protocols or theoretical formulations. The latter method is broadly based on the principle of stochastic aerodynamics. Aerodynamic theory expresses the self-excited wind forces and then uses the structural dynamics of the bridge to arrive at the buffeting response [21]. The work of Berchio and Gazzola (2015) and Yu-liang et al. (2024) forms the basis of the current theory [22]. Nevertheless, we cannot establish an explicitly ideal analytical formulation for obtaining the buffeting response of bridges due to the random behavior of atmospheric turbulence.

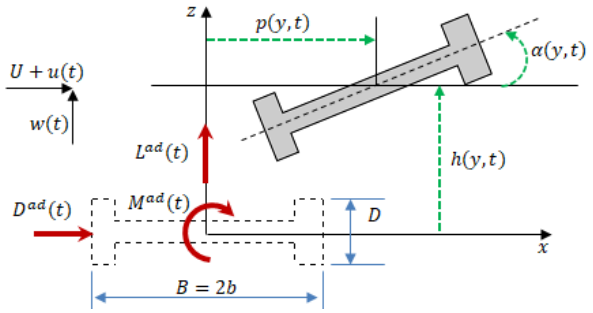

[Fig.3: Cross-Section of the old Tacoma Bridge Deck and Aerodynamic Forces Acting on it]

Based on the above assumptions [23], the system of equations of motion of the bridge deck interacting with turbulent wind according to Tang et al. (2017) is

$$[M^s]\{\ddot{q}(t)\} + [C^s]\{\dot{q}(t)\} + [K^s]\{q(t)\} = \{F_{ae}(\bar{U}, \dot{q}, q, \omega)\} + \{F_{buff}(t)\} \quad \ldots (1)$$

In the time domain, bridge flutter and buffeting are modeled using time-dependent differential equations that describe the bridge's dynamic response. Neglecting the static effect of wind, these equations include : the structural mass matrix $[M^s]$ the structural damping matrix $[C^s]$ and the structural stiffness matrix $[K^s]$. Float aeroelastic forces $\{F_{ae}(\bar{U}, \dot{q}, q, \omega)\}^T = \{D^{ae}, L^{ae}, M^{ae}\}$ and the time-dependent aerodynamic effects of turbulent wind $\{F_{buff}(t)\}$ are expressed for each nodal displacement vector $\{q\}^T = \{p, h, \alpha\}$ at mean wind speed $\bar{U}$ and reduced frequency $k = \omega b/\bar{U}$ as follows,

Retrieval Number: 100.1/ijese.K997413111024
DOI: 10.35940/ijese.K9974.13020125
Journal Website: www.ijese.org

Published By:
Blue Eyes Intelligence Engineering
and Sciences Publication (BEIESP)

$$D^{ae} = \frac{\rho\bar{U}^2 B}{2}\left(KP_1^*\frac{\dot{h}}{\bar{U}} + KP_2^*\frac{B\dot{\alpha}}{\bar{U}} + K^2P_3^*\alpha + K^2P_4^*\frac{h}{B} + KP_5^*\frac{\dot{p}}{\bar{U}} + K^2P_6^*\frac{p}{B}\right) \quad \dots (2a)$$

$$L^{ae} = \frac{\rho\bar{U}^2 B}{2}\left(KH_1^*\frac{\dot{h}}{\bar{U}} + KH_2^*\frac{B\dot{\alpha}}{\bar{U}} + K^2H_3^*\alpha + K^2H_4^*\frac{h}{B} + KH_5^*\frac{\dot{p}}{\bar{U}} + K^2H_6^*\frac{p}{B}\right) \quad \dots (2b)$$

$$M^{ae} = \frac{\rho\bar{U}^2 B^2}{2}\left(KA_1^*\frac{\dot{h}}{\bar{U}} + KA_2^*\frac{B\dot{\alpha}}{\bar{U}} + K^2A_3^*\alpha + K^2A_4^*\frac{h}{B} + KA_5^*\frac{\dot{p}}{\bar{U}} + K^2A_6^*\frac{p}{B}\right) \quad \dots (2c)$$

Where, ρ is the air density, ω is the vibration frequency of the structure and P_i^*, H_i^* and A_i^* with $i \in \{1,2,..6\}$ are the aerodynamic coefficients of the system. The aerodynamic forces (2) can be redefined with convolution integrals as noted in Amrita et al. (2024) [24].

$$D_{ae}(t) = \frac{1}{2}\rho\bar{U}^2\int_{-\infty}^{t}\left[I_{D_{ae}}^{p}(t-\tau)p(\tau) + I_{D_{ae}}^{h}(t-\tau)h(\tau) + I_{D_{ae}}^{\alpha}(t-\tau)\alpha(\tau)\right]d\tau \quad \dots (3a)$$

$$L_{ae}(t) = \frac{1}{2}\rho\bar{U}^2\int_{-\infty}^{t}\left[I_{L_{ae}}^{p}(t-\tau)p(\tau) + I_{L_{ae}}^{h}(t-\tau)h(\tau) + I_{L_{ae}}^{\alpha}(t-\tau)\alpha(\tau)\right]d\tau \quad \dots (3b)$$

$$M_{ae}(t) = \frac{1}{2}\rho\bar{U}^2\int_{-\infty}^{t}\left[I_{M_{ae}}^{p}(t-\tau)p(\tau) + I_{M_{ae}}^{h}(t-\tau)h(\tau) + I_{M_{ae}}^{\alpha}(t-\tau)\alpha(\tau)\right]d\tau \quad \dots (3c)$$

Where I represents the impulse function of self-excited forces, which are related to independent aerodynamic functions, as used by Strømmen and Hjorth-Hansen (1995) [25], Wang et al. (2011) [26]. By performing the Fourier transform of (3) and comparing it with the corresponding terms in (2), we can determine the link between the aerodynamic impulse functions (e.g. $\bar{I}_{D_{ae}}^{p}$ is the Fourier transform of $I_{D_{ae}}^{p}(t-\tau)$) and float derivatives, as follows

$$\begin{aligned}
\bar{I}_{D_{ae}}^{p} &= 2k^2(P_6^* + iP_5^*) & \bar{I}_{L_{ae}}^{\alpha} &= 2k^2b(H_3^* + iH_2^*)\\
\bar{I}_{D_{ae}}^{\alpha} &= 2k^2b(P_3^* + iP_2^*) & \bar{I}_{M_{ae}}^{p} &= 2k^2(A_6^* + iA_5^*)\\
\bar{I}_{D_{ae}}^{h} &= 2k^2(P_4^* + iP_1^*) & \bar{I}_{M_{ae}}^{h} &= 2k^2(A_4^* + iA_1^*) \quad \dots (4)\\
\bar{I}_{L_{ae}}^{p} &= 2k^2(H_6^* + iH_5^*) & \bar{I}_{M_{ae}}^{\alpha} &= 2k^2b^2(A_3^* + iA_2^*)\\
\bar{I}_{L_{ae}}^{h} &= 2k^2(H_4^* + iH_1^*) & .
\end{aligned}$$

Approximate forms are developed for the aeroelastic forces as continuous functions as a function of reduced frequency k for further analysis. Roger's approximation approach can be adopted for this purpose, Lystad et al. (2020) [27]. As an example, the term corresponding to lift induced by vertical motion $\bar{I}_{L_{ae}}^{h}(i\omega)$ its aerodynamic transfer function is expressed by

$$\bar{I}_{L_{ae}}^{h}(i\omega) = A_1 + A_2\left(\frac{i\omega b}{\bar{U}}\right) + A_3\left(\frac{i\omega b}{\bar{U}}\right)^2 + \sum_{n=1}^{N}\frac{A_{n+3}i\omega}{i\omega + d_n\bar{U}/b} \quad \dots (5)$$

The coefficients A_1, A_2, A_3, A_{n+3} and $d_n (d_n \geq 0$ and $n \in \{1,2,..,N\})$ behave as constants with respect to frequency, where, A_1 and A_2 are the static aerodynamic and damping terms respectively the term A_3 term represents the added aerodynamic mass, and the unstable components following the velocity term are represented by the rational terms, which allow us to estimate time delays using positive values of the parameter d_n.

Let $s = (-\xi + i)\omega$ with ξ is the damping ratio, then, using an inverse Laplace transform, the aerodynamic impulse function is as follows

$$I_{L_{ae}}^{h} = A_1\delta(t) + A_2\left(\frac{b}{\bar{U}}\right)\dot{\delta}(t) + A_3\left(\frac{b}{\bar{U}}\right)^2\ddot{\delta}(t) + \sum_{n=1}^{N}\int_{-\infty}^{t}A_{n+3}\exp\left(-\frac{d_n\bar{U}}{b}(t-\tau)\delta(\tau)\right)d\tau \quad \dots (6)$$

Consequently, the self-excited lift caused by random vertical motion can be written as

$$I_{L_{ae}}^{h} = \frac{1}{2}\rho\bar{U}^2\left(A_1h(t) + A_2\left(\frac{b}{\bar{U}}\right)\dot{h}(t) + A_3\left(\frac{b}{\bar{U}}\right)^2\ddot{h}(t) + \sum_{n=1}^{N}\phi_n(t)\right) \quad \dots (7)$$

The new variables introduced to express the aerodynamic offset are $\phi_n(t), n \in \{1,2,..,N\}$ so as to satisfy

$$\dot{\phi}_n(t) = -\frac{d_n\bar{U}}{b}\phi_n(t) + A_{n+3}h(t), n \in \{1,2,..,N\} \quad \dots (8)$$

For the sake of brevity, expressions for other self-excited force components are not included here, but can be supplied with comparable definitions.

Based on convolution integrals involving aerodynamic impulse functions and variable wind speeds, unit buffeting forces are generated as follows

$$D_{buff}(t) = -\frac{1}{2}\rho\bar{U}^2\int_{-\infty}^{t}\left[I_{D_{buff}}(t-\tau)\frac{u(\tau)}{\bar{U}} + I_{D_{buff}}(t-\tau)\frac{w(\tau)}{\bar{U}}\right]d\tau \quad \dots (9b)$$

$$L_{buff}(t) = -\frac{1}{2}\rho\bar{U}^2\int_{-\infty}^{t}\left[I_{L_{buff}}(t-\tau)\frac{u(\tau)}{\bar{U}} + I_{L_{buff}}(t-\tau)\frac{w(\tau)}{\bar{U}}\right]d\tau \quad \dots (9b)$$

$$M_{buff}(t) = -\frac{1}{2}\rho\bar{U}^2\int_{-\infty}^{t}\left[I_{M_{buff}}(t-\tau)\frac{u(\tau)}{\bar{U}} + I_{M_{buff}}(t-\tau)\frac{w(\tau)}{\bar{U}}\right]d\tau \quad \dots (9b)$$

Where I denotes the aerodynamic impulse expression for buffeting forces and u and w are the x- and z-direction components of random wind speed, respectively. The buffeting forces can then be expressed as follows

$$D_{buff}(t) = -\frac{1}{2}\rho\bar{U}^2(2b)\left(2C_D\chi_{L_{buff}}^{u}\frac{u(t)}{\bar{U}} + \frac{dC_D}{d\alpha}\chi_{D_{buff}}^{w}\frac{w(t)}{\bar{U}}\right) \dots (10a)$$

$$L_{buff}(t) = -\frac{1}{2}\rho\bar{U}^2(2b)\left(2C_L\chi_{L_{buff}}^{u}\frac{u(t)}{\bar{U}} + \left(\frac{dC_L}{d\alpha} + C_D\right)\chi_{D_{buff}}^{w}\frac{w(t)}{\bar{U}}\right) \dots (10b)$$

$$M_{buff}(t) = -\frac{1}{2}\rho\bar{U}^2(2b)^2\left(2C_M\chi_{M_{buff}}^{u}\frac{u(t)}{\bar{U}} + \frac{dC_M}{d\alpha}\chi_{M_{buff}}^{w}\frac{w(t)}{\bar{U}}\right) \dots (10c)$$

With, C_D, C_L and C_M are the static aerodynamic coefficients of the system (wind bridge) and the aerodynamic admittances $\chi_{D_{buff}}^{u}, \chi_{D_{buff}}^{w}, \chi_{L_{buff}}^{u}, \chi_{L_{buff}}^{w}, \chi_{M_{buff}}^{u}$ and $\chi_{M_{buff}}^{w}$.

Frequency-dependent random wind forces can be integrated into the time analysis in the same way as aeroelastic forces. Here's a relationship between the aerodynamic transfer functions and the Fourier transform of the aerodynamic impulse functions of the buffeting forces

$$\bar{I}^{u}_{D_{buff}} = 4bC_D\chi^{u}_{D_{buff}} \quad \bar{I}^{w}_{D_{buff}} = 4b\frac{dC_D}{d\alpha}\chi^{w}_{D_{buff}}$$
$$\bar{I}^{u}_{L_{buff}} = 4bC_L\chi^{u}_{L_{buff}} \quad \bar{I}^{w}_{L_{buff}} = 2b\left(\frac{dC_L}{d\alpha} + C_D\right)\chi^{w}_{L_{buff}} \dots \quad (11)$$
$$\bar{I}^{u}_{M_{buff}} = 8b^2C_M\chi^{u}_{M_{buff}} \quad \bar{I}^{w}_{M_{buff}} = 4b^2\frac{dC_M}{d\alpha}\chi^{w}_{M_{buff}}$$

On the basis of the above, it is possible to express these values as rational functions. For example, the lift induced by vertical wind fluctuation $L^{w}_{buff}(t)$

$$\bar{I}^{w}_{L_{buff}}(t) = A_{w,1} + \sum_{n=1}^{N_w}\frac{A_{w,n+1}i\omega}{i\omega + d_{w,n}\bar{U}/b} \quad \dots \quad (12)$$

Next, we can calculate the lift due to buffeting caused by a random fluctuation in the vertical wind as follows

$$L^{w}_{buff} = -\frac{1}{2}\rho\bar{U}^2\left(\left(A_{w,1} + A_{w,2}\right)\frac{w(t)}{\bar{U}} - \sum_{n=1}^{N_w}\frac{d_{w,n}\bar{U}}{b}\phi_{w,n}(t)\right) \dots \quad (13)$$

$$\dot{\phi}_{w,n}(t) = -\frac{d_{w,n}\bar{U}}{b}\phi_{w,n}(t) + A_{n+1}\frac{w(t)}{\bar{U}}, n \in \{1,2,..,N_w\} \dots \quad (14)$$

For the sake of brevity, comparable formulas for other components of the turbulence force are not included here. The portion of lift and buffeting applied over the entire bridge span of length L can be expressed as

$$L^{L}_{ae}(t) = \int_{x=0}^{x=L} L_{ae}(t)dx \quad L^{L}_{buff}(t) = \int_{x=0}^{x=L} L_{buff}(t)dx \quad \dots \quad (15)$$

By the same method, the associated drag and moment can be given. The stochastic characteristics of the buffeting forces per unit length of the bridge at various points on the same element are assumed to be the same as those defined at the center of the element, while the correlation between the buffeting force components caused by fluctuations u(t) and w(t) is neglected. Consequently, the self-excited and buffeting forces across the element are defined as follows

$$L^{e}_{ae}(t) = L^{c}_{ae}(t)L \quad \dots \quad (16)$$
$$L^{e}_{buff}(t) = L\int_0^t\left(\Gamma^{u}_{L_{buff}}(t-\tau)L^{c}_{buff}(\tau) + \Gamma^{w}_{L_{buff}}(t-\tau)L^{c}_{buff}(\tau)\right)d\tau \quad \dots \quad (17)$$

With, the superscript "c" indicates the center of the element and $\Gamma^{u}_{L_{buff}}$ and $\Gamma^{w}_{L_{buff}}$ are the impulse functions with these Fourier transforms $\bar{\bar{\Gamma}}^{w}_{L_{buff}}$ and $\bar{\bar{\Gamma}}^{w}_{L_{buff}}$ also known as joint acceptance functions, expressed as follows

$$\bar{\bar{\Gamma}}^{w}_{L_{buff}} = \sqrt{\frac{1}{L^2}\int_0^L\int_0^L coh^{w}_{L_{buff}}(y_1,y_2,f)dy_1dy_2} \quad \dots \quad (18)$$

With $coh^{w}_{L_{buff}}(y_1,y_2,f) = S^{w}_{L_{buff}}(y_1,y_2,f)/S^{c}_{L_{buff}}(f)$ gives the coherence of the component of the buffeting lift force $L^{w}_{L_{buff}}$ and $S^{w}_{L_{buff}}(y_1,y_2,f)$ is the two-position cross-spectrum of the span y_1 and y_2 and finally the spectral density of $L^{c}_{L_{buff}}(f)$ is $S^{c}_{L_{buff}}(f)$.

Using Beta-Newmark's step-by-step integration procedure to find the solutions to the equations of motion. Let's start with the construction of the aerodynamic forces. First, the wind fluctuation in the middle of each element has been presented. Taking into account the previous expressions, the aerodynamic forces applied to each element have been calculated, and then we assemble the nodal vectors $\{F_{ae}(\bar{U},\dot{q},q,\omega)\}$ and $\{F_{buff}(t)\}$. On the other hand, the self-excited aerodynamic forces depend on the unknown vibrations of the bridge, so an iterative procedure is mandatory for each time step.

C. Solving the Problem

In order to select the most significant modes for motion, a modal approach is required. In a generalized coordinate system $\{q\}$ in the modal basis $[\Phi]$the equations of motion (1) become

$$[\Phi]^T[M^s][\Phi]\{\ddot{q}\} + [\Phi]^T[C^s][\Phi]\{\dot{q}\} + [\Phi]^T[K^s][\Phi]\{q\} = [\Phi]^T\{F_{ae}\} + [\Phi]^T\{F_{buff}\} \quad \dots \quad (19)$$

System (19) can be written in a more compact form as follows

$$[M]\{\ddot{q}\} + [C]\{\dot{q}\} + [K]\{q\} = \{Q_{ae}\} + \{Q_{buff}\} \quad \dots \quad (20)$$

Shifting the self-excited force term in (20) to the left and writing the generalized self-excited forces as the two matrices A_s and A_s depend on frequency

$$Q_{ae} = \frac{1}{2}\rho\bar{U}^2\left(A_s q + A_d\frac{b}{\bar{U}}\dot{q}\right) \quad \dots \quad (21)$$

In rational form, the generalized aeroelastic forces can be written as

$$\{Q_{ae}(i\omega)\} = A_s + \left(\frac{i\omega b}{\bar{U}}\right)A_d = A_1 + A_2\left(\frac{i\omega b}{\bar{U}}\right) + A_3\left(\frac{i\omega b}{\bar{U}}\right)^2 + \sum_{n=1}^{N}\frac{A_{n+3}i\omega}{i\omega + d_n\bar{U}/b} \quad \dots \quad (22)$$

The coefficients A_1, A_2, A_3, A_{n+3} and $d_n (d_n \geq 0\ and\ n \in \{1,2,..,N\})$ behave as constants with respect to frequency. Applying the Laplace transform $(s = i\omega)$ on systems (20) and (21) and substituting (22), we obtain

$$s^2[\bar{\bar{M}}]q(s) = \{-s[\bar{\bar{C}}] - [\bar{\bar{K}}]\}q(s) + \frac{1}{2}\rho U^2\sum_{n=1}^{N}\{q_n^{ae}(s)\} + \{Q_{buff}(s)\} \quad \dots \quad (23)$$

With,

$$[\bar{\bar{M}}] = [M] - 0.5\rho b^2A_3$$
$$[\bar{\bar{C}}] = [C] - 0.5\rho b\bar{U}A_2 \quad \dots \quad (24a)$$
$$[\bar{\bar{K}}] = [K] - 0.5\rho\bar{U}^2A_1$$

$$\{q_n^{ae}(s)\} = \frac{A_{n+3}s}{s + d_n\bar{U}/b}\{q(s)\};\ n \in \{1,2,..,N\} \quad \dots \quad (24b)$$

By performing the inverse Laplace transformation, the

set of equations of motion of the system formatted as a state space can be written as follows:

$$\{\dot{X}\} = [A]\{X\} + [B]\{Q_{buff}\} \quad \dots \quad (25)$$

With,

$$\{X\}^T = \{q, q, q_1^{ae}, q_2^{ae}, \dots\dots, q_N^{ae}\} \quad \dots \quad (26a)$$

$$[A] = \begin{bmatrix} 0 & I & 0 & \dots & 0 \\ -[\bar{M}]^{-1}[\bar{K}] & -[\bar{M}]^{-1}[\bar{C}] & \frac{1}{2}\rho\bar{U}^2[\bar{M}]^{-1} & \dots & \frac{1}{2}\rho\bar{U}^2[\bar{M}]^{-1} \\ 0 & A_4 & -\frac{\bar{U}}{b}d_1 I & \dots & 0 \\ \vdots & \vdots & \vdots & \ddots & \vdots \\ 0 & A_{N+3} & 0 & \dots & -\frac{\bar{U}}{b}d_N I \end{bmatrix} \dots (26b)$$

$$[B]^T = \left[0, [\bar{M}]^{-1}, 0, \dots\dots, 0\right] \quad \dots \quad (27)$$

The above state-space equation as a function of time can be examined in a numerical integration technique to study both the buffeting reaction and the floating instability in the time domain. A Beta-Newmark algorithm is used for this purpose. To extract frequencies, damping ratios and mode shapes from the free vibration response, the effects of the buffeting force can be ignored when analyzing aeroelastic vibrations.

III. NUMERICAL RESULTS AND INTERPRETATION

Table 1 illustrates the geometric and mechanical properties of the old Tacoma Bridge deck, as well as the aerodynamic properties of the wind-bridge system, inspired by references Jurado and Hernandez (2004) [28], Sebastiano et al. (2023) [29].

Table 1 : Main Structural and Aerodynamic Properties of the old Tacoma Bridge

Structural and Material Property	Value
Length of main span (m)	446
Beam mass (kg/m)	5350
Mass of main cables (kg/m)	408
Mass moment of inertia (kg m^2 /m)	82.43
Deck height (m)	2.76
Deck width (m)	12.3
Static Aerodynamic Properties	**Value**
C_D Drag coefficient	1.0
C_L Lift coefficient	0.1
C_M Moment coefficient	0.02
$dC_D/d\alpha$ 1ère derived from drag coefficient	0.0
$dC_L/d\alpha$ 1ère derived from the departure coeffi.	3.0
$dC_M/d\alpha$ 1ère derived from moment coeff.	1.12

A. Modal Parameters of the old Tacoma Bridge and Validation of the Formulation

Before looking at the bridge's dynamic response, a modal analysis is generally carried out to identify the natural frequencies and the modal basis. {Φ}. Natural frequencies are the frequencies at which the bridge enters resonance, i.e. where it vibrates with maximum amplitude in response to buffeting excitation. In Table 2, the first nine natural frequencies of the lateral, vertical and torsional movements of the old Tacoma Bridge have been determined. Based on several MATLAB program extracts, a multitude of natural modes have been determined, but they are not implemented below for the sake of brevity.

We propose the following meanings, L: lateral, V: vertical and T: means torsion, symmetrical natural modes are noted S: and A: means asymmetrical.

Table 2 : Eigenfrequencies of the old Tacoma Bridge Compared to the Literature

Mode	Present	Ref*	Δf(%)	Mode	Present	Ref*	Δf(%)	Mode	Present	Ref*	Δf(%)
HS1	0.0816	0.0811	+0.61	VA1	0.1373	0.1364	-0.68	TS1	0.5873	0.5812	-1.03
HA1	0.1616	0.1626	-0.61	VS1	0.2684	0.2681	-0.17	TA1	1.1185	1.1174	-0.09
HS2	0.2956	0.2941	-0.32	VS2	0.3614	0.3610	-0.15	TS2	1.6768	1.6761	-0.04

*Jurado J. A. and Hernandez S. (2004) [28]

Table 2 includes values obtained by other researchers, showing a better agreement between the frequencies calculated with the present formulation and those identified by Jurado and Hernandez (2004) [28].

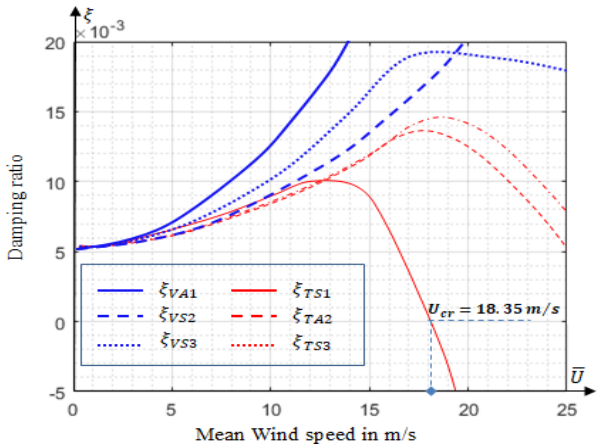

[Fig.4: Evolution of Overall Modal Damping of the old Tacoma Bridge as a Function of Average Speed]

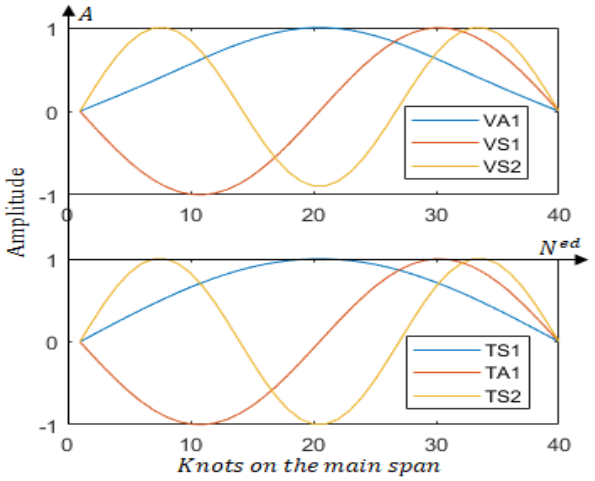

[Fig.5: First Three Modes of Vertical and Torsional Vibration]

In Figure 4, the damping corresponding to torsion mode TS1 is the one that crosses the horizontal axis first, indicating

that a zero damping value has been reached. As a result, pure torsional instability will be induced. In the case of the old Tacoma Bridge, a one-dimensional torsional instability is induced before transverse bending.

The resulting critical wind speed for the pure torsional instability of this bridge is $U_{cr} = 18.35\ m/s$which is very close to that measured in the field on the day of collapse $(19m/s)$, as provided by Farquharson (1949) in reference Liu et al. (2020) [30]. While Figure 5 shows the first three vertical and torsional eigenmodes.

B. Turbulent wind Generation

In order to examine the impact of the coupling of buffeting and aeroelastic forces on suspension bridge instability, the production of stochastic wind records is crucial. It must be stressed that the use of field measurement and prediction tools is very costly and not accessible to everyone. From this point of view, my idea in this study was to use computational fluid dynamics (CFD) tools to produce random series representing turbulent wind over a 15mn time interval, in particular concerning the nature of random winds on the topographic site of the former Tacoma Bridge, and to exploit them theoretically to predict the dynamic response of the bridge, then to compare them with field results found in the literature [31]. In particular, the algorithms and procedures followed by Xu and Moan (2018)

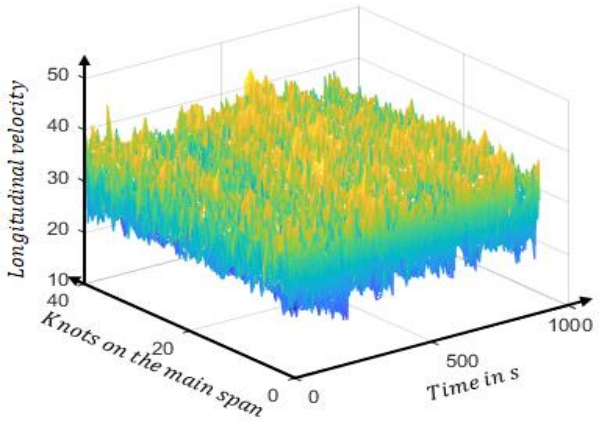

[Fig.6: Longitudinal Wind Statistics for an Average of 30m/s]

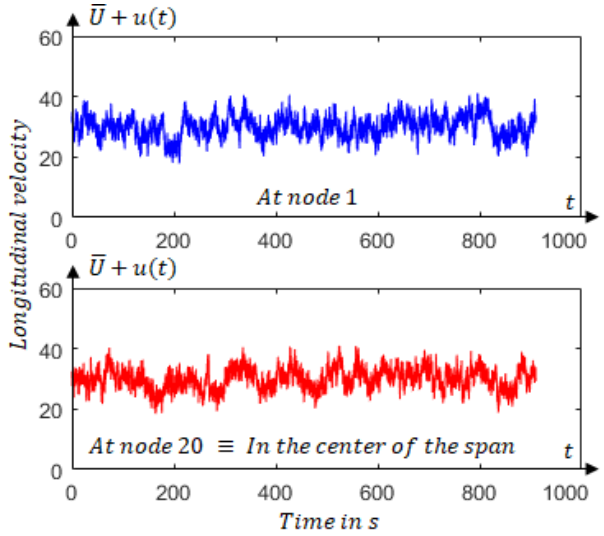

[Fig.7: Chronogram of Longitudinal Wind Speed at Two Nodes of the Main Span]

The turbulent wind field has been generated and represented in terms of disturbed velocity intensity in Figures 6, 7, 8 and 9. We choose a range of wind speeds from 10m/s to 30m/s, and this is imposed by the critical wind speed that led to the collapse of the Tacoma Bridge due to aerodynamic instability as found in section 3.1.

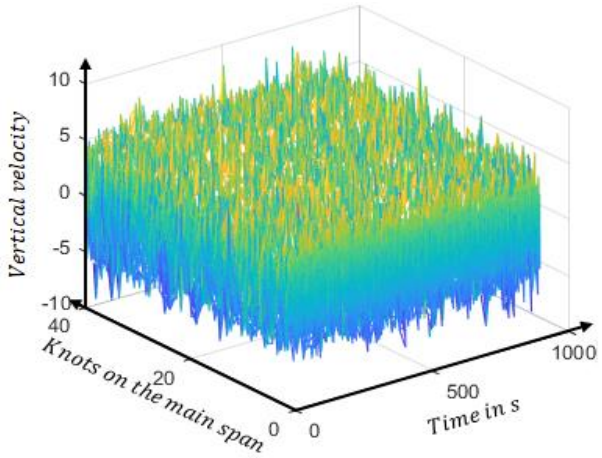

[Fig.8: Vertical Wind Statistics for an Average of 0m/s]

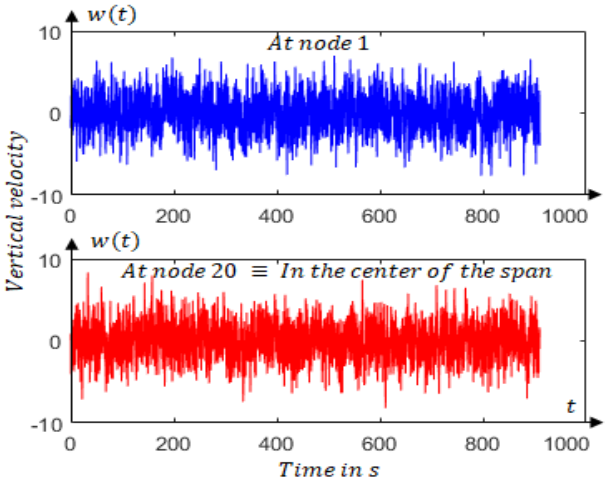

[Fig.9. Chronogram of Longitudinal wind Speed at two Nodes of the Main Span]

In Figures 6 and 8, the average wind speed is shown in conjunction with these turbulent components, with Figure 6 showing the representation of horizontal winds with an average speed of 30 meters per second, while Figure 8 shows only turbulent wind speeds without the average speed. In figures 7 and 9, the wind is represented at two different points along the bridge

C. Case Study: Dynamic Response of the old Tacoma Bridge to Turbulent Winds

The spectral frequency response of the old Tacoma Bridge is a representation of how the structure reacts to wind excitation forces at different frequencies [32]. It shows the amplitude of vibrations (vertical and torsional) of the structure for each excitation frequency, as shown in Figures 10 and 12 (respectively). Figures 11 and 13 show vertical and angular displacements over time, respectively [33].

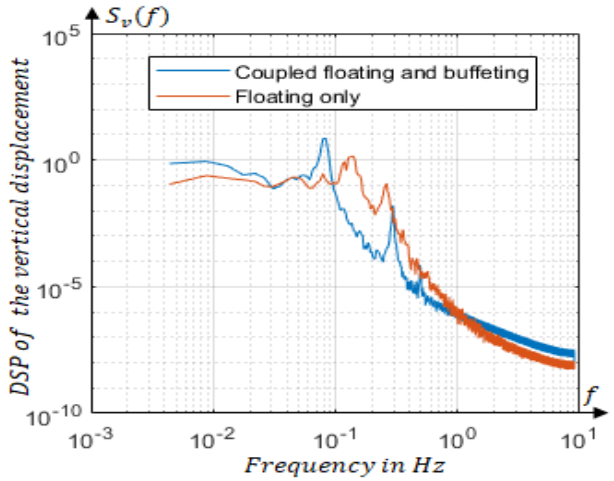

[Fig.10. Spectral Response to Vertical Displacement in the Middle of the Main Span]

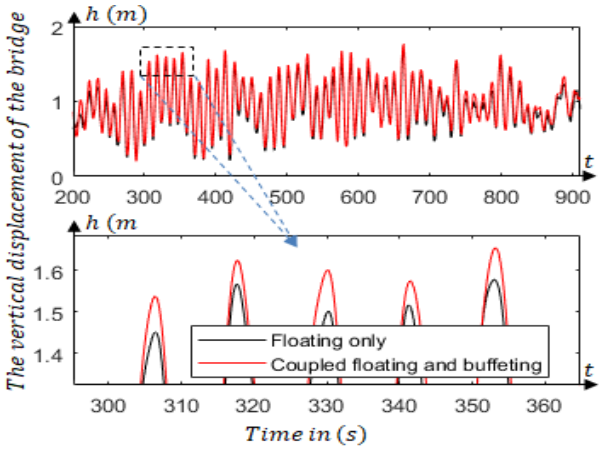

[Fig.11. Vertical Dynamic Response in the Middle of the Main Span Over Time]

Figure 10 shows the vertical displacement response of the bridge in the two cases of floating alone (in red) and floating coupled with the buffeting effect (in blue). Let's start with the behavior of floating alone, which shows two peaks, the first at a frequency of 0.14Hz and the second at 0.26Hz. The two peaks in the spectral response curve correspond to the natural frequencies of vertical bridge vibrations, where the risk of resonance is high. But when the buffeting effect is coupled to the bridge's dynamic behavior (blue curve), the bridge's vertical resonance peaks shift to 0.08Hz and 0.29Hz respectively [34].

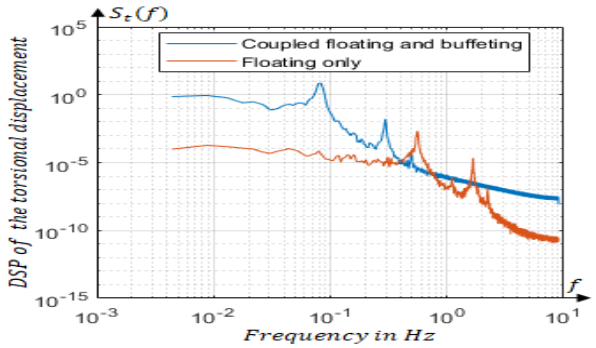

[Fig.12: Spectral Response to Vertical Displacement in the Middle of the Main Span]

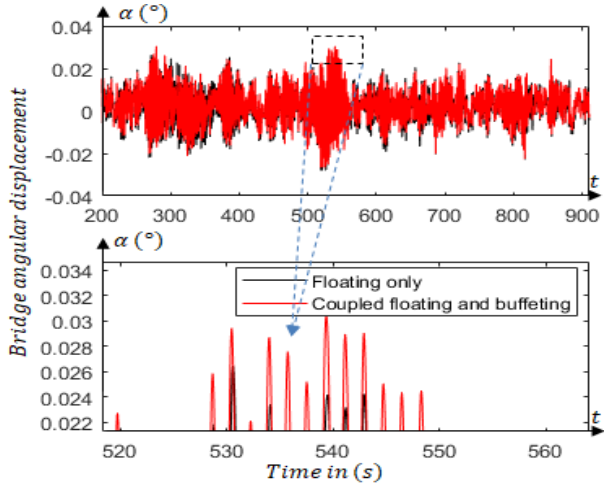

[Fig.13: Dynamic Torsional Response in the Middle of the Main Span Over Time]

We conclude that the effect of buffeting does not necessarily increase or decrease frequencies according to a specific pattern, but rather can increase or decrease frequencies. Consequently, engineers must take into account the random nature of turbulent winds when determining the resonance potential of bridge structure vibrations. Based on the same figure, we conclude that the effect of buffeting vibrations increases vibration amplitude, as confirmed in Figure 11. The same conclusions can be drawn from Figures 13 and 14, which represent the torsional oscillations of the bridge deck in the presence of random winds, but in this case it turns out that the coupling of buffeting with flutter has a greater impact on increasing the amplitude of torsional oscillations.

Figures 14 and 15 show the standard deviation (RMS) of the Tacoma bridge's vertical and torsional acceleration response, respectively. The responses are determined in frequency and time domain for both coupled and uncoupled cases. We conclude that the coupling of buffeting effects has the effect of increasing the standard deviation, especially at high speeds.

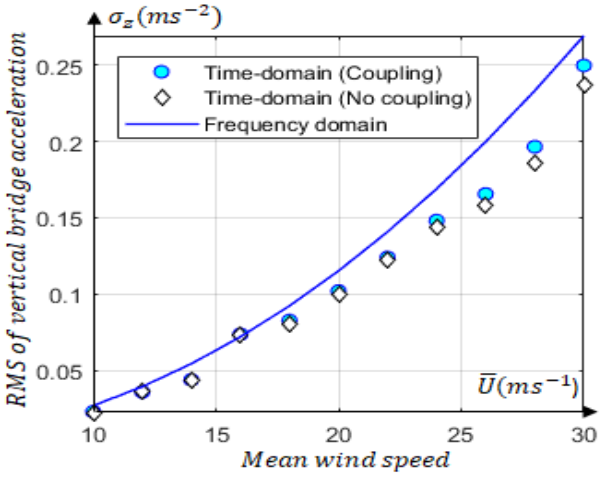

[Fig.14: Standard Deviation of Vertical Bridge Acceleration as a Function of Mean wind Speed]

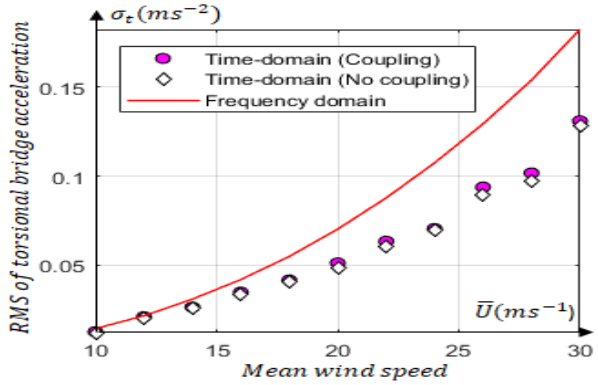

[Fig.15: Standard Deviation of Bridge Torsional Acceleration as a Function of Mean Wind Speed]

The standard deviation of the frequency response quantifies the dispersion of response amplitudes around their mean value for each excitation frequency. A high standard deviation indicates greater variability in bridge response, which may point to resonance zones or complex dynamic phenomena.

D. Parametric Studies

Parametric studies enable us to understand how different parameters (study domain, damping, turbulence, etc.) affect the bridge's dynamic responses. In Figures 16 and 17 we have plotted the spectral frequency and time-domain vertical and torsional acceleration response of the bridge, respectively, for a mean wind speed of 30m/s. The two figures show that the two studies correspond to each other in terms of time and frequency, or at least that they work in the same way to highlight the phenomenon of potential resonance.

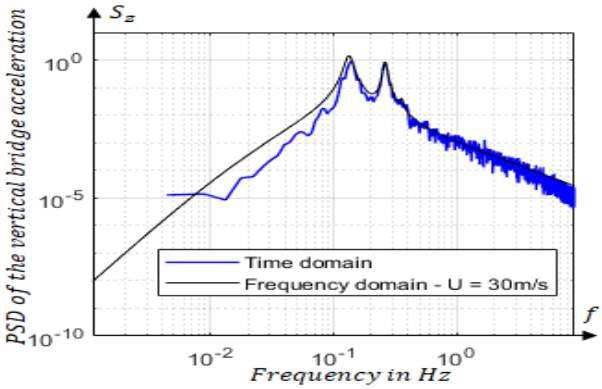

[Fig.16: Spectral and Time Response in Vertical Bridge Acceleration]

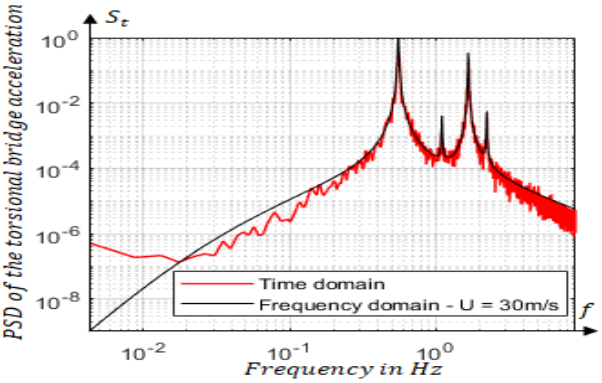

[Fig.17: Spectral and Time Response to Bridge Torsional Acceleration]

Thanks to parametric studies, engineers can explore different design and material configurations to minimize the effects of buffeting. The result is more robust designs that better withstand adverse wind conditions.

Figures 18 and 19 show the impact of the structural damping ratio on the spectral response to vertical and torsional acceleration, respectively.

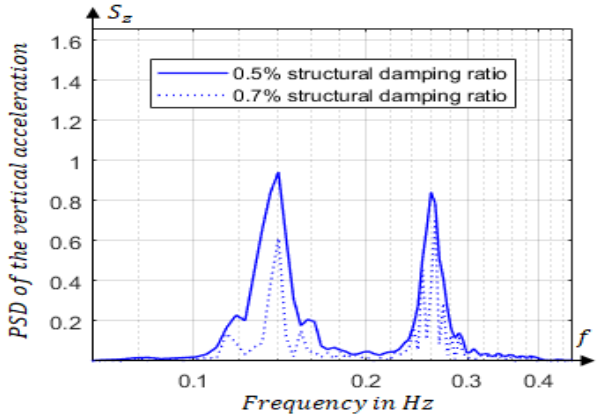

[Fig.18: Effect of Structural Damping on Vertical Spectral Displacement Response]

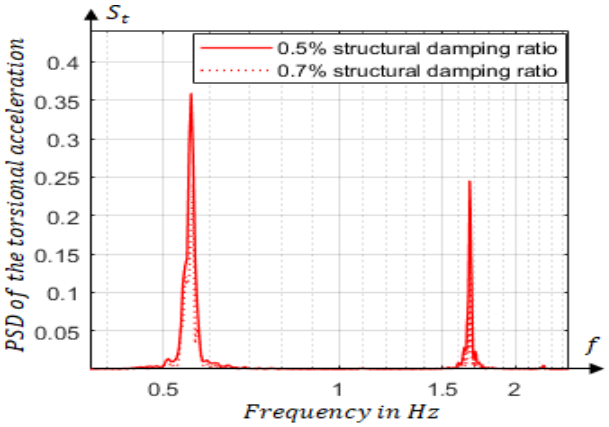

[Fig.19: Effect of Structural Damping on Torsional Displacement Spectral Response]

By analyzing the spectral response of the two figures, we can understand how energy is dissipated in the system, which is essential for assessing the effectiveness of damping devices (such as tuned-mass dampers) installed on the bridge. The need for such a system is based on observing the reaction of the bridge structure to changes in its damping system. Figures 18 and 19 show that the more powerful the structure's damping system, the weaker the bridge's response to random winds.

In short, buffeting analysis of suspension bridges is essential to ensure their safety and durability. By combining frequency- and time-domain analysis methods, engineers can better understand the effects of turbulent winds and design bridges capable of resisting these forces. Preventive and control measures, such as improving aerodynamic design and installing damping devices, are essential to minimize the impact of buffeting and ensure the optimum performance of suspension bridges.

Retrieval Number: 100.1/ijese.K997413111024
DOI: 10.35940/ijese.K9974.13020125
Journal Website: www.ijese.org

Published By:
Blue Eyes Intelligence Engineering and Sciences Publication (BEIESP)

IV. CONCLUSIONS

The effects of turbulent winds on suspension bridges are significant, and can have a significant impact on the floating instability of the bridge, and consequently on its safety and performance. Here are some key conclusions regarding these effects, starting with the impact on suspension bridge stability, turbulent winds can induce oscillations and vibrations in suspension bridges, including torsional and vertical bending movements. These oscillations can be self-sustaining, resulting in amplified vibrations that can damage the structure. At wind speeds close to or above the critical floating speed, the oscillations caused can be amplified by buffeting forces. Conversely, buffeting forces can influence the development of flutter, by modifying the speed at which it occurs or the nature of the oscillations induced. This coupling can make the structure's behavior very difficult to predict and control, as it can lead to unstable oscillations that increase steadily over time. Damping is a key factor in dissipating vibrations caused by buffeting. Adequate damping reduces the intensity and duration of oscillations, minimizing the risk to the structure. Dynamic dampers can be integrated into the design to improve overall bridge damping.

ACKNOWLEDGEMENTS

The support given to this research project by the Université Sidi Mohamed Ben Abdellah de Fès is gratefully acknowledged. The authors would also like to thank the professors at ENS Fès for their help in correcting the manuscript.

DECLARATION STATEMENT

After aggregating input from all authors, I must verify the accuracy of the following information as the article's author.

- **Conflicts of Interest/ Competing Interests:** Based on my understanding, this article has no conflicts of interest.
- **Funding Support:** This article has not been funded by any organizations or agencies. This independence ensures that the research is conducted with objectivity and without any external influence.
- **Ethical Approval and Consent to Participate:** The content of this article does not necessitate ethical approval or consent to participate with supporting documentation.
- **Data Access Statement and Material Availability:** The adequate resources of this article are publicly accessible.
- **Authors Contributions:** Each author has individually contributed to the article - Hafid MATAICH: Bibliographical research, formulation + Programming, - Bouchta EL AMRANI: bibliographical research, linguistic correction + translation

REFERENCES

1. Yi Su, Jin Di, Shaopeng Li, Bin Jian and Jun Liu (2022); Buffeting Response Prediction of Long-Span Bridges Based on Different Wind Tunnel Test Techniques; *Applied Sciences*, ***12***(6), 3171; DOI : https://doi.org/10.3390/app12063171
2. Brownjohn J. M. W. and Jakobsen J. B. (2001); Strategies for aeroelastic parameter identification from bridge deck free vibration data; Journal of Wind Engineering and Industrial Aerodynamics, 89(13), 1113-1136; DOI : https://doi.org/10.1016/S0167-6105(01)00091-5
3. Defang Chen, Weiwei Wang, H. Elhosiny Ali, Amjad S. Qazaq and Minghui Long (2024); Vibration/bending analysis of waist twisting disc with three-layer circular magnetic porous micro-plate in sports equipments during exercise ; Geomechanics and Engineering, An International Journal, Volume 39, Number 5, pages 425-439; https://www.techno-press.org/content/?page=article&journal=gae&volume=39&num=5&ordernum=1
4. Lorenzo Raffaele, Gertjan Glabeke and Jeroen van Beeck (2023); Wind-sand tunnel experiment on the windblown sand transport and sedimentation over a two-dimensional sinusoidal hill ; Wind and Structures, Volume **36**, Number 2 pages 075-90; https://www.techno-press.org/content/?page=article&journal=was&volume=36&num=2&ordernum=1
5. Zhang J., Zhou L., Tian Y., Yu S., Zhao W. and Cheng, Y. (2021); Vortex-induced vibration measurement of a long-span suspension bridge through noncontact sensing strategies ; Computer-Aided Civil and Infrastructure Engineering ; Volume 37, Issue 12 Pages 1617-1633; DOI : https://doi.org/10.1111/mice.12712
6. Hua X., Wang C., Li S. and Chen, Z. (2020); Experimental investigation of wind-induced vibrations of main cables for suspension bridges in construction phases; Journal of Fluids and Structures, 93, 102846; DOI : https://doi.org/10.1016/j.jfluidstructs.2019.102846
7. Xia J., Li K. and Ge Y. (2020); Wind tunnel testing and frequency domain buffeting analysis of a 5000 m suspension bridge; Advances in Structural Engineering, Volume 24, Issue 7 Pages 1326-1342; DOI : https://doi.org/10.1177/1369433220975568
8. Hafid Mataich and Bouchta El Amrani (2023); The Impact of Flexural/Torsional Coupling on the Stability of Symmetrical Laminated Plates ; European Journal of Computational Mechanics, Vol. 32 5, pages 441–466 ; DOI : https://doi.org/10.13052/ejcm2642-2085.3251
9. Li M., Li M. and Sun Y. (2021); Effects of turbulence integral scale on the buffeting response of a long-span suspension bridge; Journal of Sound and Vibration, 490, 115721; DOI : https://doi.org/10.1016/j.jsv.2020.115721
10. Hu L. and Xu Y.-L. (2014); Extreme value of typhoon-induced non-stationary buffeting response of long-span bridges; Probabilistic Engineering Mechanics, 36, 19 27; DOI : https://doi.org/10.1016/j.probengmech.2014.02.002
11. Tang H., Li Y. and Shum, K. (2017); Flutter performance of long-span suspension bridges under non-uniform inflow; Advances in Structural Engineering, 21(2), 201-213; DOI : https://doi.org/10.1177/1369433217713926
12. Shuyang Cao and Jinxin Cao (2017); Toward Better Understanding of Turbulence Effects on Bridge Aerodynamics; Sec. Wind Engineering and Science Vol. **3;** DOI : https://doi.org/10.3389/fbuil.2017.00072
13. H. Mataich, A. El Amrani , J. El Mekkaoui and B. El Amrani (2024); Effect of flexure/extension coupling on the elastic instability of a composite laminate plate ; Structural Engineering and Mechanics, Vol. 90, No. 4 pages 391-401 ; DOI : https://doi.org/10.12989/sem.2024.90.4.391
14. Fenerci A., Øiseth O. and Rønnquist A. (2017); Long-term monitoring of wind field characteristics and dynamic response of a long-span suspension bridge in complex terrain; Engineering Structures, 147, 269-284; DOI : http://dx.doi.org/10.1016/j.engstruct.2017.05.070
15. Cheynet E., Jakobsen J. B., and Snæbjörnsson J. (2016); Buffeting response of a suspension bridge in complex terrain; Engineering Structures, 128, 474-487; DOI : http://dx.doi:10.1016/j.engstruct.2016.09.060 https://www.semanticscholar.org/paper/Buffeting-response-of-a-suspension-bridge-in-Cheynet-Jakobsen/96ad5171c1bd33f15726e60fd601ae85f7e73cb6
16. Weichao Liu, Peng Xu, Guangqing Yang and Miren Rong (2024) ; Seismic stability of MSE walls with stepped reinforcement arrangement subjected to vertical and horizontal accelerations ; Geomechanics and Engineering, An International Journal, Volume 39, Number 5, pages 503-512; DOI : https://doi.org/10.12989/gae.2024.39.5.503 https://www.techno-press.org/content/?page=article&journal=gae&volume=39&num=5&ordernum=6
17. Arioli G. and Gazzola, F. (2017); Torsional instability in suspension bridges: The Tacoma Narrows Bridge case; Communications in Nonlinear Science and Numerical Simulation, 42, 342-357; DOI : https://doi.org/10.1016/j.cnsns.2016.05.028
18. Ammann O.H., Von Karman T., Woodruff GB (1941); The failure of the Tacoma Narrows Bridge; Washington D.C.: Federal Works Agency. https://authors.library.caltech.edu/records/q1ehq-5e206
19. Scanlan R. H. (1978); The action of flexible bridges under wind, II: Buffeting theory ; Journal of Sound and Vibration, 60(2), 201-211; DOI : https://doi.org/10.1016/S0022.460X(78)80029.7
20. Scanlan R. W. H. (1982); Developments in Low.Speed Aeroelasticity in the Civil

Engineering Field; AIAA Journal, 20(6), 839-844; DOI : https://doi.org/10.2514/3.51141
21. Berchio E. and Gazzola F. (2015); A qualitative explanation of the origin of torsional instability in suspension bridges; Nonlinear Analysis: Theory, Methods & Applications, **121**, 54-72; DOI : https://doi.org/10.1016/j.na.2014.10.026
22. Yu-liang Lin, Li Lu, Hao Xing, Xi Ning and Li-hua Li (2024) ; Upper bound solution on seismic anchor force and earth pressure of a combined retaining structure ; Geomechanics and Engineering, An International Journal, Volume 39, Number 2, pages 171-179; DOI : https://doi.org/10.12989/gae.2024.39.2.171
23. Tao T., Wang H. and Wu T. (2017); Parametric study on buffeting performance of a long-span triple-tower suspension bridge; Structure and Infrastructure Engineering, 14(3), 381-399; DOI : https://doi.org/10.1080/15732479.2017.1354034
24. Amrita, B.R. Jayalekshmi and R. Shivashankar (2024) ; Dynamic stability evaluation of nail stabilised vertical cuts in various site classes ; Geomechanics and Engineering, An International Journal, Volume 39, Number 2, pages 421-437; DOI : https://doi.org/10.12989/gae.2024.38.4.421
25. Strømmen E. and Hjorth-Hansen E. (1995); The buffeting wind loading of structural members at an arbitrary attitude in the flow ; Journal of Wind Engineering and Industrial Aerodynamics, 56(2-3), 267-290; DOI : https://doi.org/10.1016/0167-6105(94)00092-R
26. Wang H, Li A, Hu R. (**2011**); Comparison of ambient vibration response of the runyang suspension bridge under skew winds with time-domain numerical predictions. J Bridge Eng, 16(4):513-26; DOI : http://dx.doi.org/10.1061/(ASCE)BE.1943-5592.0000168
27. Lystad T. M., Fenerci A. and Øiseth O. (2020); Buffeting response of long-span bridges considering uncertain turbulence parameters using the environmental contour method; Engineering Structures, 213, 110575; DOI : https://doi.org/10.1016/j.engstruct.2020.110575
28. Jurado J. A. and Hernandez S. (2004) ; Sensitivity analysis of bridge flutter with respect to mechanical parameters of the deck ; Structural and Multidisciplinary Optimization, 27(4), 272-283; DOI : https://doi.org/10.1007/s00158-003-0374-8
29. Sebastiano Russo, Gianfranco Piana , Luca Patruno and Alberto Carpinteri (2023) ; Preliminary Flutter Stability Assessment of the Double-Deck George Washington Bridge ; Appl. Sci., **13**, 6389. DOI : https://doi.org/10.3390/app13116389
30. Liu S., Cai C. S. and Han Y. (2020); Time-domain simulations of turbulence effects on the aerodynamic flutter of long-span bridges; Advances in Bridge Engineering, **1**(1); DOI : https://doi.org/10.1186/s43251-020-00007-6
31. Xu Y., Øiseth O. and Moan T. (2018); Time domain simulations of wind- and wave-induced load effects on a three-span suspension bridge with two floating pylons; Marine Structures, 58, 434-452; DOI : https://doi.org/10.1016/j.marstruc.2017.11.012
32. Hadimani, S., Diwakar, Dr. N., Selokar, Dr. G. R., & Rao, Dr. B. N. (2021). Design & Analysis of Dynamic Response in Hydrolic Equipment Working with Heavy Loads. In International Journal of Engineering and Advanced Technology (Vol. 10, Issue 3, pp. 215–218). DOI : https://doi.org/10.35940/ijeat.c2243.0210321
33. Sangeetha K, Vimala S, Research on Laterally Restrained Built Up Steel Beam Under Dynamic Response. (2019). In International Journal of Innovative Technology and Exploring Engineering (Vol. 8, Issue 6S4, pp. 1057–1061). DOI : https://doi.org/10.35940/ijitee.f1218.0486s419
34. K.Saravanan, L.Porchelvi, K. Selvakumar, Hysteresis Controlled Quadratic Boost Converter Based AC Micro Grid System with Improved Dynamic Response. (2019). In International Journal of Recent Technology and Engineering (Vol. 8, Issue 2S11, pp. 3327–3337). DOI : https://doi.org/10.35940/ijrte.b1561.0982s1119

AUTHOR'S PROFILE

He is **Mataich Hafid**, and he'scurrently a PhD student in Civil Engineering, specializing in Structural Mechanics, with a particular focus on Continuous Media Mechanics. My research work is carried out within the Mathematics, Modeling and Applied Physics laboratory, at the Sidi Mohamed Ben Abdellah University of Fez, affiliated with the École Normale Supérieure de Fez, Morocco. As part of my doctoral studies, I am interested in the analysis and modeling of complex mechanical behaviors of structures and materials under various constraints, with a view to developing innovative solutions to improve the design and sustainability of modern infrastructures.

Professor Bouchta El Amrani, holder of a chair in applied mathematics, is a member of the Laboratory of Mathematics, Modeling and Applied Physics, attached to the École Normale Supérieure of the Sidi Mohamed Ben Abdellah University in Fez, Morocco. This laboratory is distinguished by its advanced research in the fields of pure and applied mathematics, as well as in the modeling of complex physical phenomena. The Sidi Mohamed Ben Abdellah University, located in Fez, is a renowned academic center, where Professor EL AMRANI conducts research that contributes to the development of science and engineering at the national and international levels.